Journal of Research in Science and Engineering (JRSE)
ISSN: 1656-1996 Volume-6, Issue-11, November 2024
DOI: 10.53469/jrse.2024.06(11).17

Modal Matching of Key Components in the Launching System Based on Response Surface Method

Yue Ma[1], Qilin Shu[2], Yuekang Yue[3]

[1]Shenyang Ligong University, School of Mechanical Engineering, Shenyang 110159, China
[2]Shenyang Ligong University, Shenyang 110159, China
[3]Shanghai DongHu Machinery Factory, Shanghai 201900, China
[1]*yuegegeya@gmail.com*

Abstract: ***This chapter adopts Response Surface Methodology (RSM) combined with dynamic simulation and statistical analysis to deeply investigate the impact of modal matching of the inherent frequencies of key components of the launching system on the disturbances at the launch box opening during firing. Through experimental design, a polynomial fitting response surface model is established between design parameters and response objectives. The ultimate goal is to find the optimal design scheme that minimizes the initial disturbance, thereby achieving effective modal matching between the main components of the launching device. This research aims to provide a theoretical basis for improving firing accuracy and system stability.***

Keywords: Response Surface Method, Modal Analysis, Harmonic Response Analysis, Modal Matching.

1. Introduction

Response Surface Methodology (RSM) is an effective statistical technique used to explore the relationship between variables and response objectives in complex systems. With the continuous advancement of Computer-Aided Engineering (CAE) technology, it is now possible to more accurately predict real-world situations through model simulations in the early stages of design. However, the complexity of real engineering problems presents greater challenges for simulation models and solving algorithms, especially in optimization design, which often requires multiple iterative calculations. This not only extends the development cycle but also increases project costs. Therefore, to reduce the workload of handling practical issues, there is an urgent need to apply mathematical statistical methods reasonably to build effective surrogate models to address complex, highly nonlinear simulation optimization problems. In this context, RSM has gained widespread attention in the engineering field and has been rapidly applied to various optimization design and reliability analysis areas.

For example, Shengyu Zeng [1] analyzed the application of response surface-based approximation methods in the parallel subspace optimization of anti-ship missile systems and proposed an optimization framework and corresponding mathematical formulations. This method replaces complex simulation models with response surface models to reduce computational load and improve optimization efficiency. In the developed framework, the design space is divided into multiple subspaces for parallel local optimization and global coordination, thus achieving efficient collaborative optimization. Mathematical examples were used in the optimization process to validate the feasibility of the parallel subspace optimization design method, proving its effectiveness and accuracy in handling complex multi-objective design problems.

Similarly, Wenkan Che [2] applied the response surface method to optimize three critical structural parameters of the hub bearing inner ring—inclination angle, slant distance, and corner radius—ultimately maximizing the ratio of the press-fit pre-tightening force to the change in the outer diameter of the inner ring. Yu-Gang Wang and Shichao Xiu [3] applied RSM to conduct multi-objective optimization on the motor bracket, focusing primarily on stress and mass as response parameters. They first established corresponding response surface models and, after completing the optimization, used simulation analysis for comparative validation of the feasibility and effectiveness of the optimized solution. In the seismic resistance analysis of short-pier cable-stayed bridges, Hongtao He [4] and others used RSM for seismic optimization design. They took the parameters of the transverse energy dissipation system as optimization objectives. They constructed a quadratic polynomial response surface model and derived the optimization scheme based on this. Finally, through simulation verification, the stability of the optimized short-pier cable-stayed bridge was significantly improved.

2. Overview of Response Surface Methodology Based on Design-Expert

The Box-Behnken design uses multivariable quadratic regression equations to accurately model the nonlinear relationship between design variables and response objectives [5]. This design method not only effectively identifies the optimal response values but also generates related charts and analysis data, which facilitate a deeper understanding of how design variables affect the response. It is suitable for experiments with 3 to 7 factors, and with its efficient number of experimental runs and accuracy, the Box-Behnken design has been widely applied in various fields. Typically, the number of experimental runs ranges from 15 to 62. First, the design variables that significantly impact the objective response need to be identified, and their value ranges are set under practical conditions. Next, an appropriate experimental design method is selected for reasonable sample collection to

construct a response surface approximation model and perform sample testing to validate the model's feasibility. Finally, based on the established polynomial model, the response values are optimized, and the optimization results are substituted into the original simulation model for computation to compare the optimization effect, thereby verifying the effectiveness of the adopted optimization strategy [6]. This process ensures the systematic and scientific nature of the optimization procedure, helping to improve the accuracy and reliability of the design [7].

3. Modal Analysis of Key Components of the Launching System

During the operation of the launching system, intense vibrations between important components such as the launch box, bracket, connecting rod, and screw are inevitable. Therefore, it is crucial to conduct an in-depth analysis of the vibration characteristics of these components. By studying the modal relationships between these key components and correlating them with the launch box opening response, appropriate optimization strategies can be adopted to reduce the mutual influence between the components. This approach will effectively reduce the vibration response at the launch box opening and significantly improve shooting accuracy and stability during continuous firing [8].

3.1 Mesh Generation and Modal Analysis of the Launch Box

The launch box is discretized using hexahedral elements. Considering that the launch box experiences significant torsional deformation during the firing process and to ensure a higher displacement accuracy, C3D8R elements are used for the mesh generation [9]- [10]. The launch box model consists of a total of 24,130 nodes and 14,329 elements. The finite element mesh model of the launch box is shown in Figure 1.

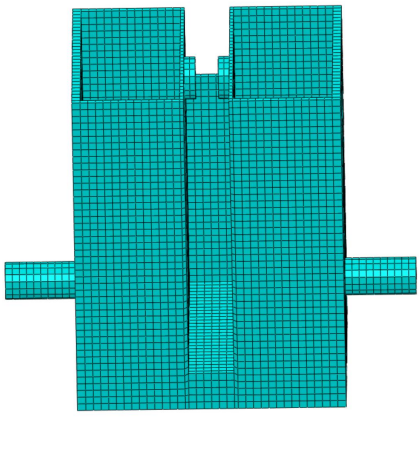

Figure 1: Finite Element Mesh Model of the Launch Box

After meshing the launch box, and considering the actual working state during the operation of the launch device, where all the connecting parts are locked during firing, fixed boundary conditions were applied to the ear pin and the central ear pin hole of the launch box. Using finite element analysis, the first six natural frequencies and their corresponding mode shapes were obtained. The specific results are detailed in Table 1 and Figure 2.

Table 1: The first six natural frequencies of the launch box

Mode	Natural Frequency (Hz)	Mode Shape
Mode 1	22.5	First-order bending of the launch box around the z-axis
Mode 2	27.85	Second-order bending of the launch box around the z-axis
Mode 3	29.99	Third-order bending of the launch box around the z-axis
Mode 4	35.94	Fourth-order bending of the launch box around the z-axis
Mode 5	37.66	Fifth-order bending of the launch box around the z-axis
Mode 6	59.53	Sixth-order bending of the launch box around the z-axis

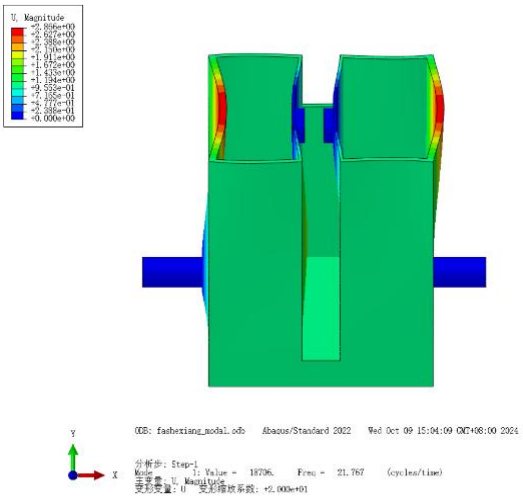

a: First-order natural frequency of the launch box

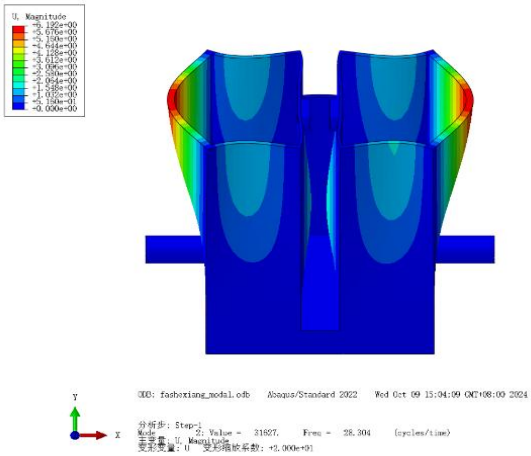

b: Second-order natural frequency of the launch box

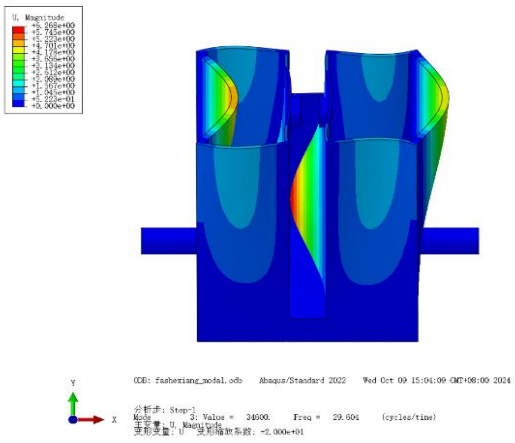

c: Third-order natural frequency of the launch box

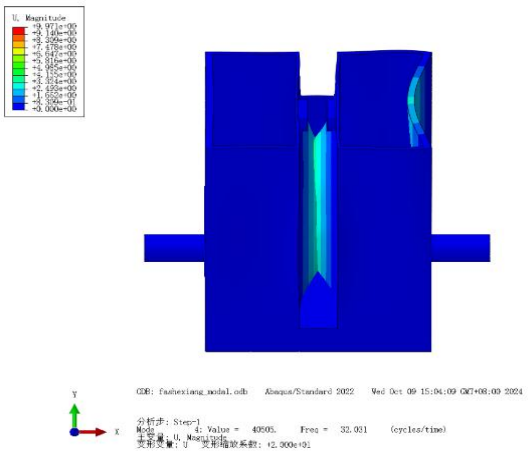

d: Fourth-order natural frequency of the launch box

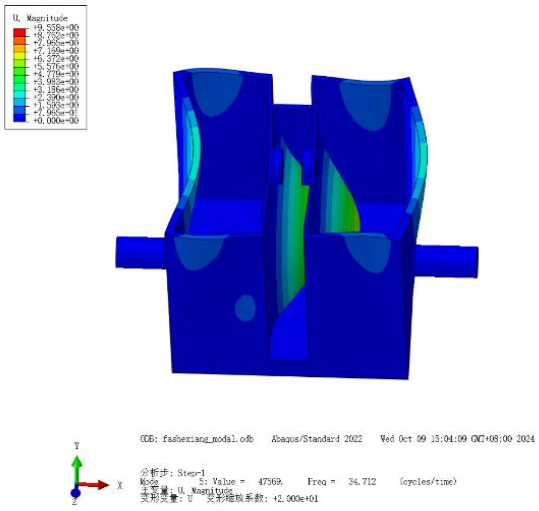

e: Fifth-order natural frequency of the launch box

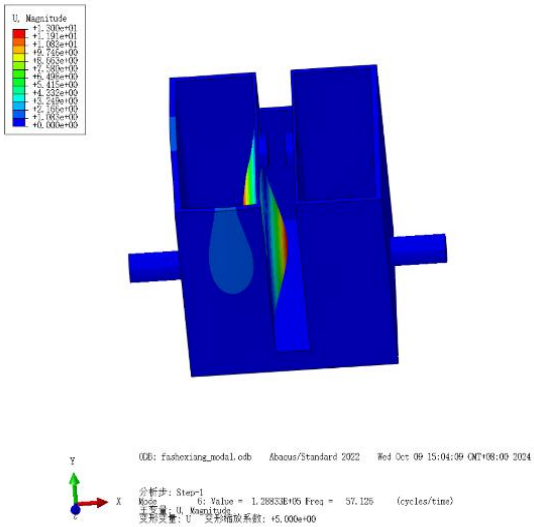

f: Sixth-order natural frequency of the launch box

Figure 2: The first six modes of the launch box

From the finite element analysis results, the first six natural frequencies of the launch box are distributed in the range of 22 Hz to 60 Hz. The first six mode shapes of the launch box reveal that there are varying degrees of displacement at the launch box opening in both the x and y directions. The third to sixth mode shapes primarily occur in the central region of the launch box. When the projectile is ejected from the launch box, any resonance in the launch box can be expected to have a significant impact on the firing accuracy.

3.2 Mesh Generation and Modal Analysis of the Bracket

Due to the complex structural characteristics of the bracket, a hybrid modeling approach is adopted, primarily using hexahedral elements. The bracket is discretized into 76,504 hexahedral elements. Considering that the bracket is the main component responsible for bearing the recoil force in the launch device, shear deformation occurs within the bracket. To prevent shear locking and obtain more accurate results, C3D8R elements are used, along with 924 tetrahedral elements, and the mesh is refined using C3D10 elements. The model consists of a total of 99,260 nodes. The finite element model of the launch box is shown in Figure 3.

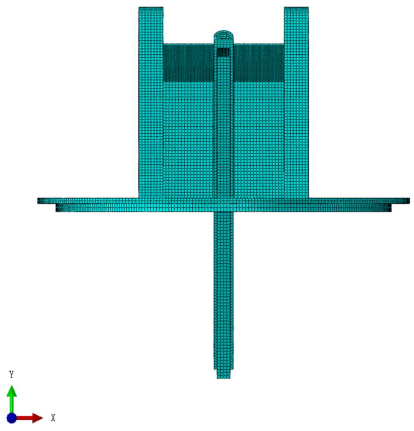

Figure 3: Finite Element Mesh Model of the Bracket

During the firing process, the bracket of the launch device is fixed to the deck, so fixed boundary conditions were applied at the bottom of the bracket to simulate the actual operating conditions. After meshing and solving, the first six natural frequencies and mode shapes of the original bracket structure were obtained. The specific data are shown in Table 2 and Figure 4.

Table 2: The first six natural frequencies of the Bracket

Mode	Natural Frequency (Hz)	Mode Shape
Mode 1	17.46	First-order longitudinal bending of the dust cover around the x-axis
Mode 2	22.95	Longitudinal bending of the screw support beam around the x-axis
Mode 3	25.68	Second-order longitudinal bending of the dust cover around the x-axis
Mode 4	26.04	Lateral bending of the screw support beam around the z-axis
Mode 5	37.56	Second-order bending of the dust cover along the z-axis
Mode 6	48.52	Third-order longitudinal bending of the dust cover around the x-axis

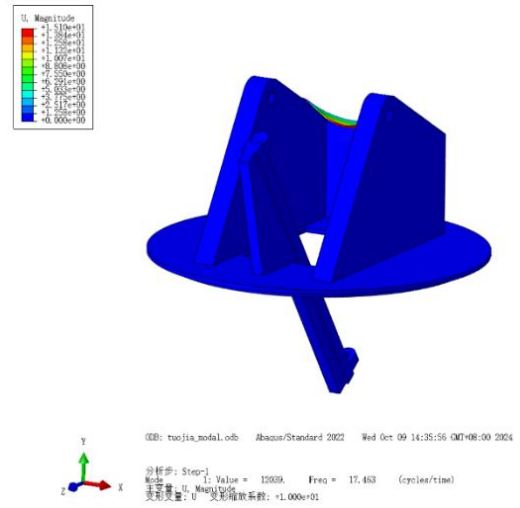

a: First-order natural frequency of the bracket

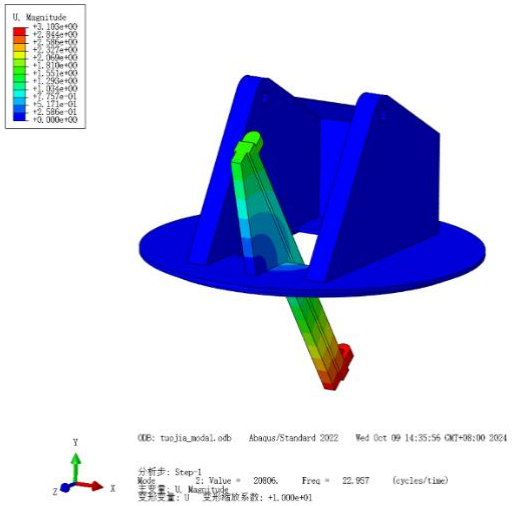

b: Second-order natural frequency of the bracket

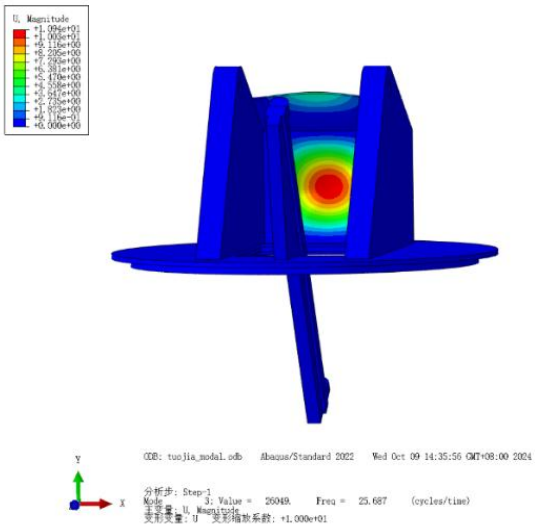

c: Third-order natural frequency of the bracket

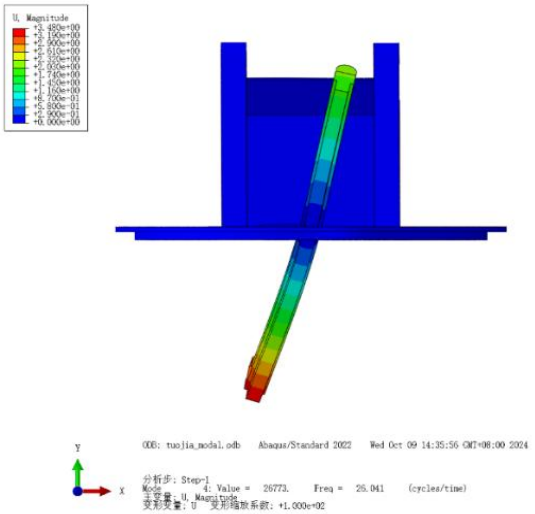

d: Fourth-order natural frequency of the bracket

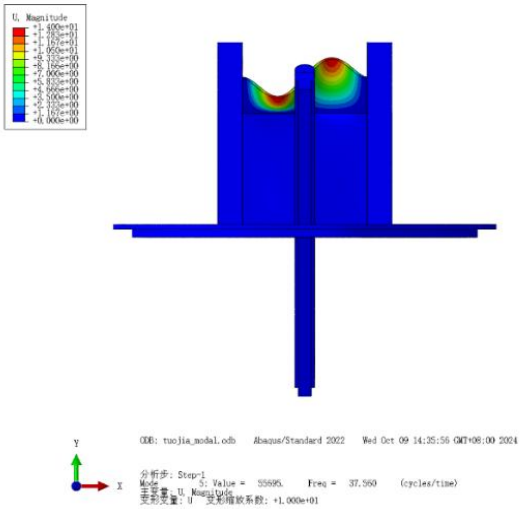

e: Fifth-order natural frequency of the bracket

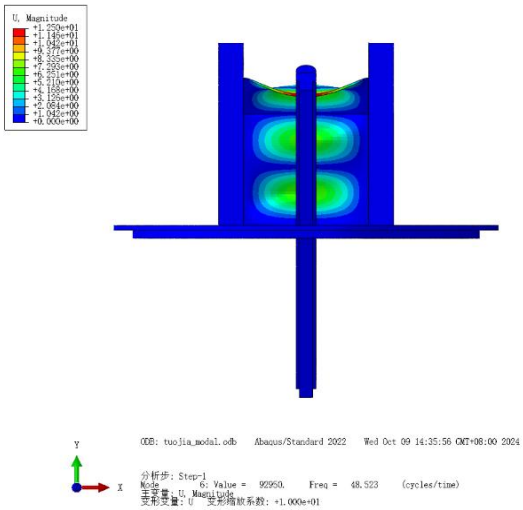

f: Sixth-order natural frequency of the bracket

Figure 4: The first six modes of the Bracket

From the finite element analysis results, the first six natural frequencies of the bracket are distributed in the range of 17 Hz to 50 Hz. The second and fourth mode shapes of the bracket show that the supporting beam of the bracket's screw experiences rotational movement around the x-axis and y-axis. The first, third, fifth, and sixth mode shapes primarily occur in the dust cover of the bracket.

3.3 Mesh Generation and Modal Analysis of the Connecting Rod

Figure 5: Finite Element Mesh Model of the connecting rod

The mesh discretization of the connecting rod is the same as that of the launch box, using C3D8R elements. The model is divided into 2,035 nodes and 1,308 elements, as shown in Figure 5.

During firing, the upper shaft hole of the connecting rod is connected and locked to the launch box through an axle, and the lower shaft hole is connected and locked to the slider through another axle. Therefore, fixed boundary conditions are applied at both shaft holes of the connecting rod according to the actual firing conditions. The first six natural frequencies of the original connecting rod structure are obtained, as shown in Table 3, and the first six mode shapes are shown in Figure 6.

Table 3: The first six natural frequencies of the connecting rod

Mode	Natural Frequency (Hz)	Mode Shape
Mode 1	405	First-order bending around the z-axis
Mode 2	638	First-order bending around the y-axis
Mode 3	1079	Second-order bending around the z-axis
Mode 4	1415	Torsion along the x-axis
Mode 5	1625	Second-order bending around the y-axis
Mode 6	2027	Third-order bending around the z-axis

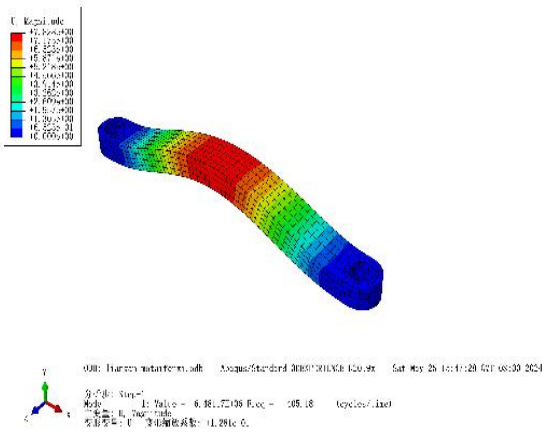

a: First-order natural frequency of the connecting rod

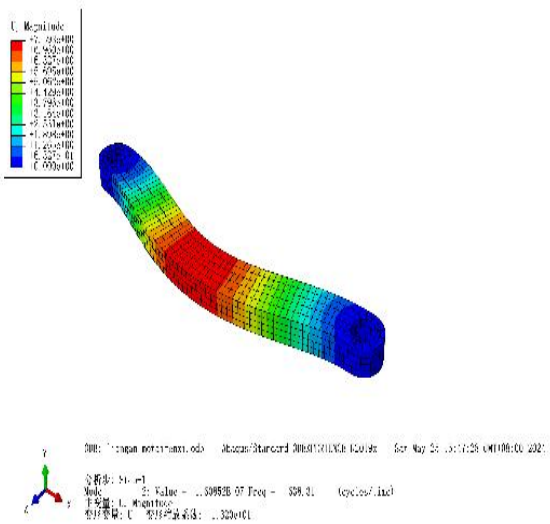

b: Second-order natural frequency of the connecting rod

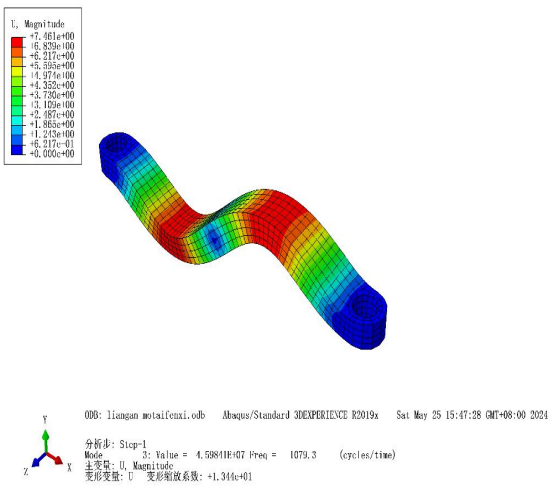

c: Third-order natural frequency of the connecting rod

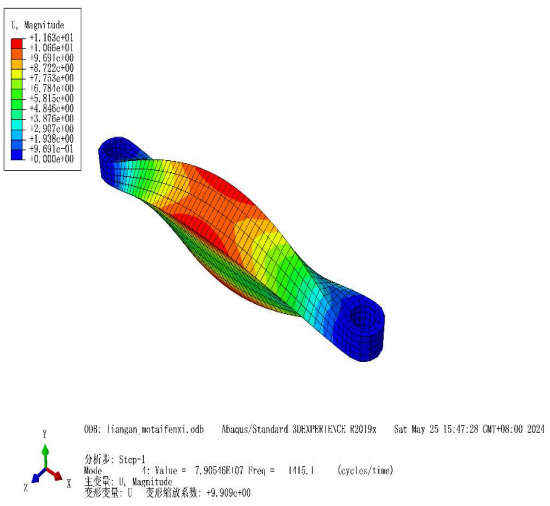

d: Fourth-order natural frequency of the connecting rod

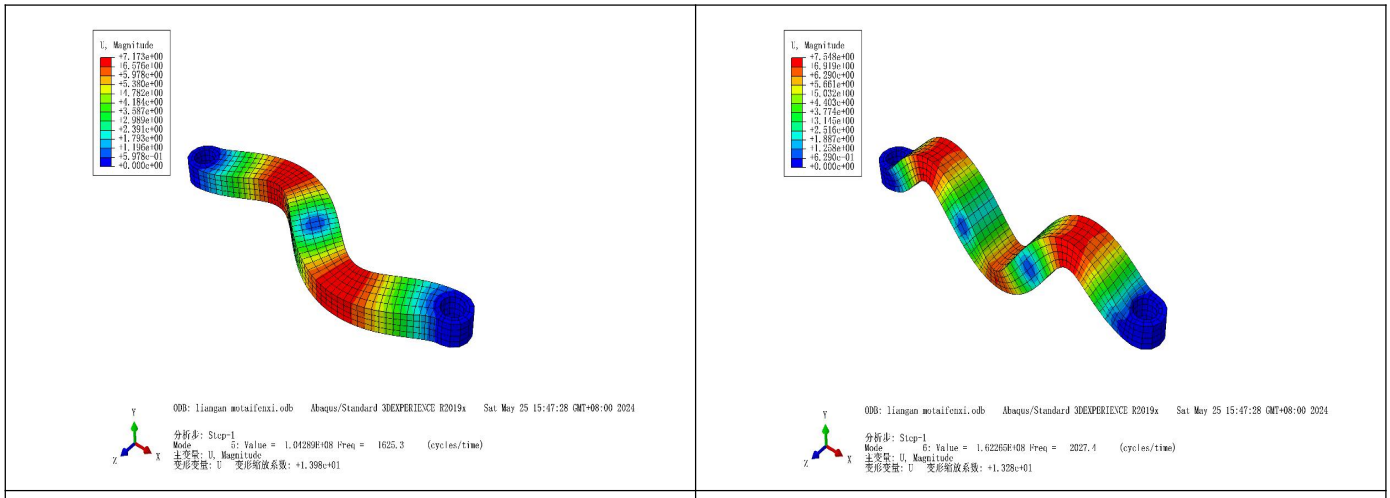

e: Fifth-order natural frequency of the connecting ro

f: Sixth-order natural frequency of the connecting rod

Figure 6: The first six modes of the connecting rod

Figure 7: Finite Element Mesh Model of the screw

From the finite element analysis results, the first six natural frequencies of the connecting rod are distributed in the range of 405 Hz to 2027 Hz. The first, third, and sixth mode shapes of the launch box correspond to the first, second, and third bending deformations of the connecting rod around the z-axis. The second and fifth mode shapes represent the first and second bending deformations of the connecting rod around the y-axis, while the fourth mode shape shows the twisting deformation of the connecting rod around the x-axis.

3.4 Mesh Generation and Modal Analysis of the Screw

The structural characteristics of the screw are relatively complex. Due to the presence of threads, it is difficult to discretize it into hexahedral elements. To ensure smoother displacement in the model, C3D10 tetrahedral elements were chosen. The model is discretized into 140,077 nodes and 93,522 elements, as shown in Figure 7.

The two ends of the screw, as well as the two ends of the screw support on the bracket, are fixed during the firing process by locking the rotational degrees of freedom of the screw. Therefore, fixed boundary conditions are applied at both ends. Modal analysis is performed, and the natural frequencies are obtained as shown in Table 4, with the mode shapes displayed in Figure 8.

Table 4: The first six natural frequencies of the screw

Mode	Natural Frequency (Hz)	Mode Shape
Mode 1	36.44	First-order bending around the z-axis
Mode 2	36.45	First-order bending around the x-axis
Mode 3	104.74	Second-order bending around the z-axis
Mode 4	104.75	Second-order bending around the x-axis
Mode 5	209.67	Third-order bending around the z-axis
Mode 6	209.69	Third-order bending around the x-axis

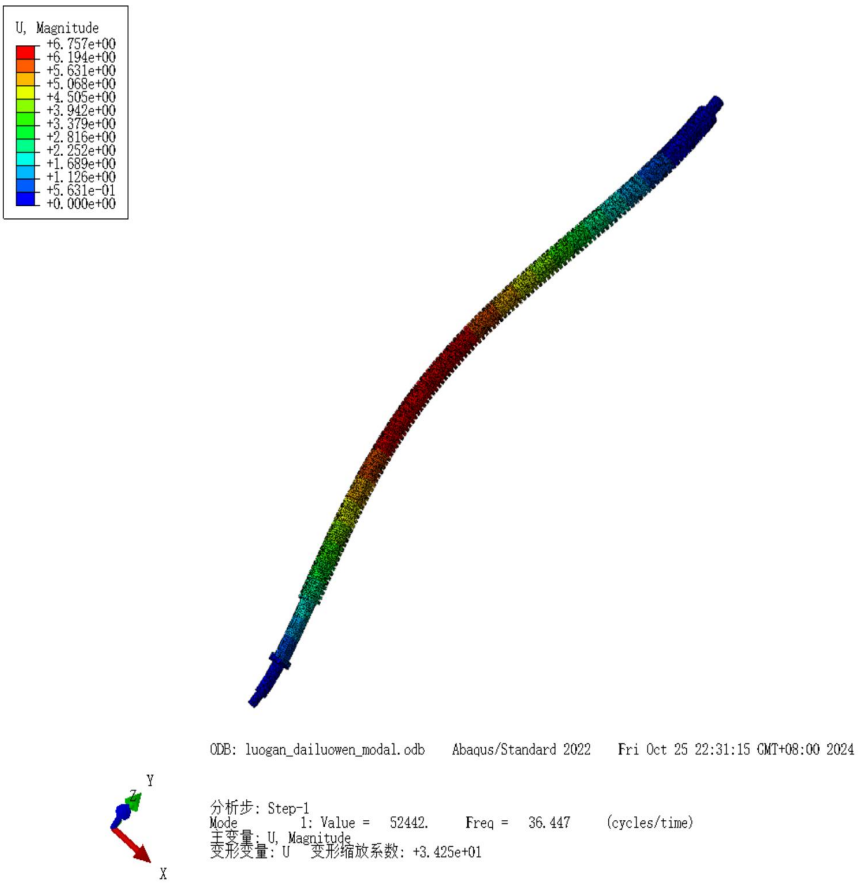

a: First-order natural frequency of the screw

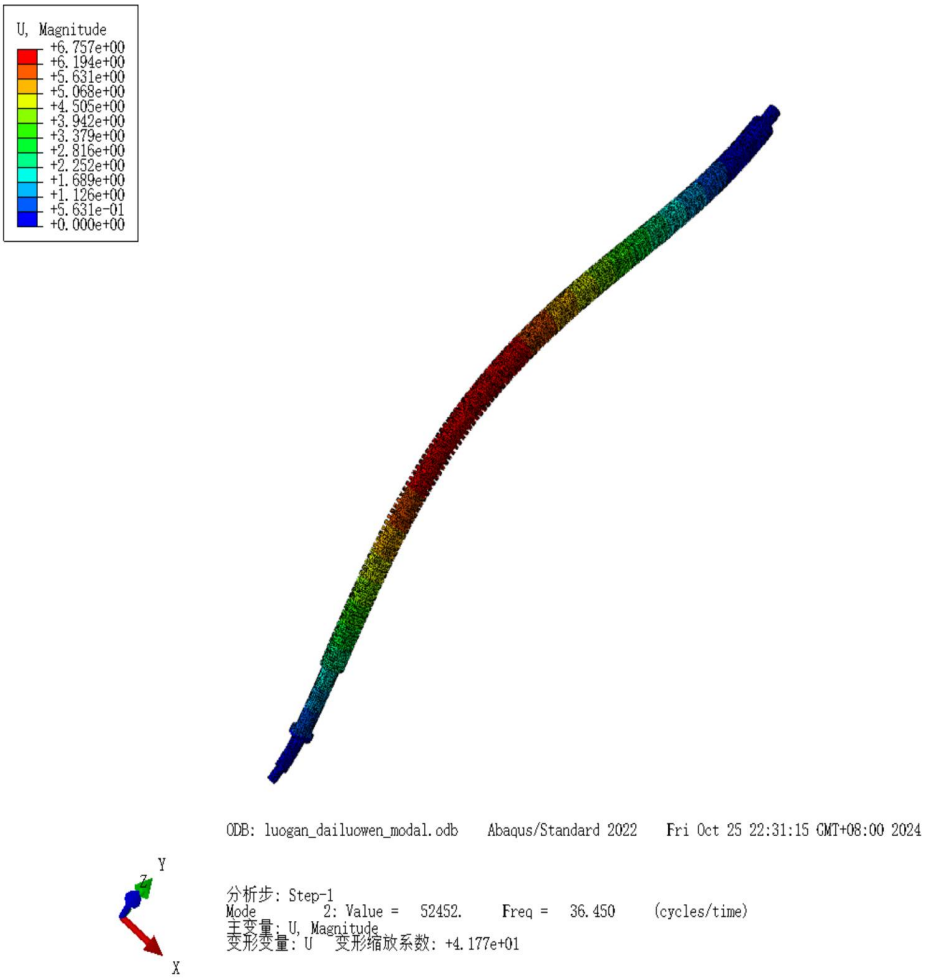

b: Second-order natural frequency of the screw

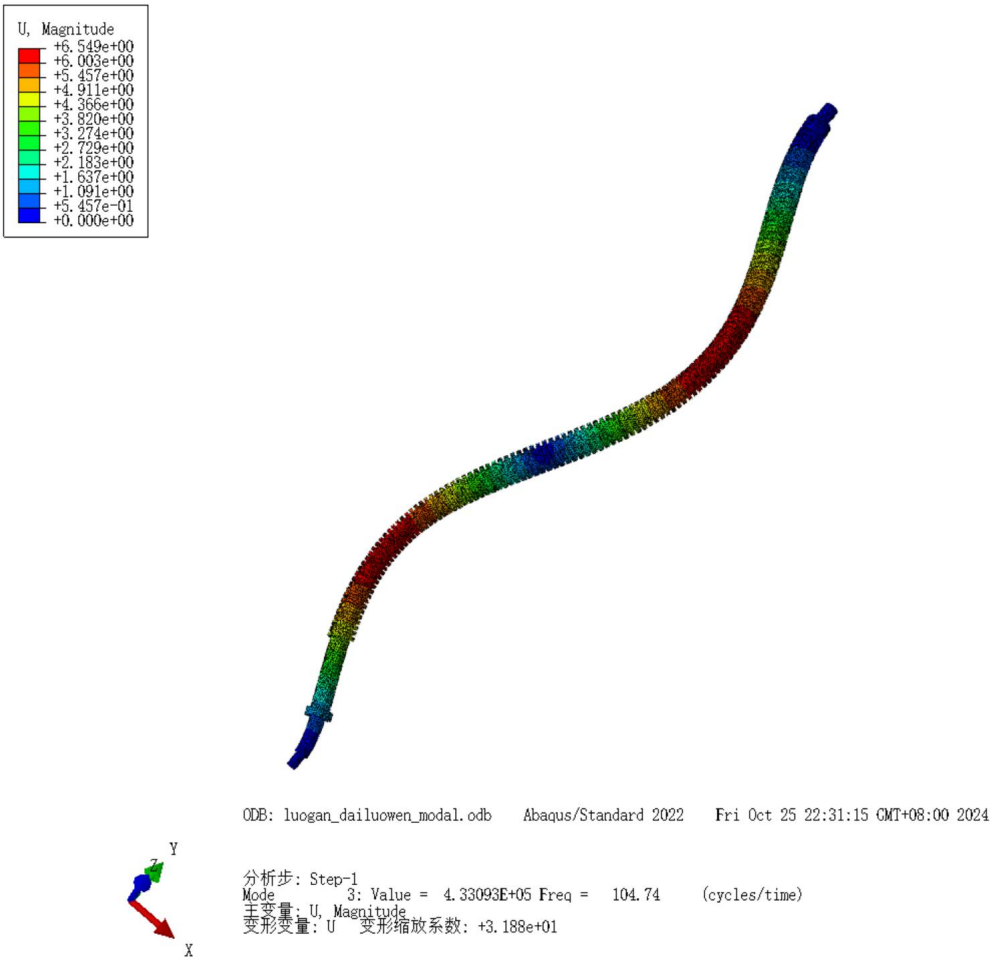

c: Third-order natural frequency of the screw

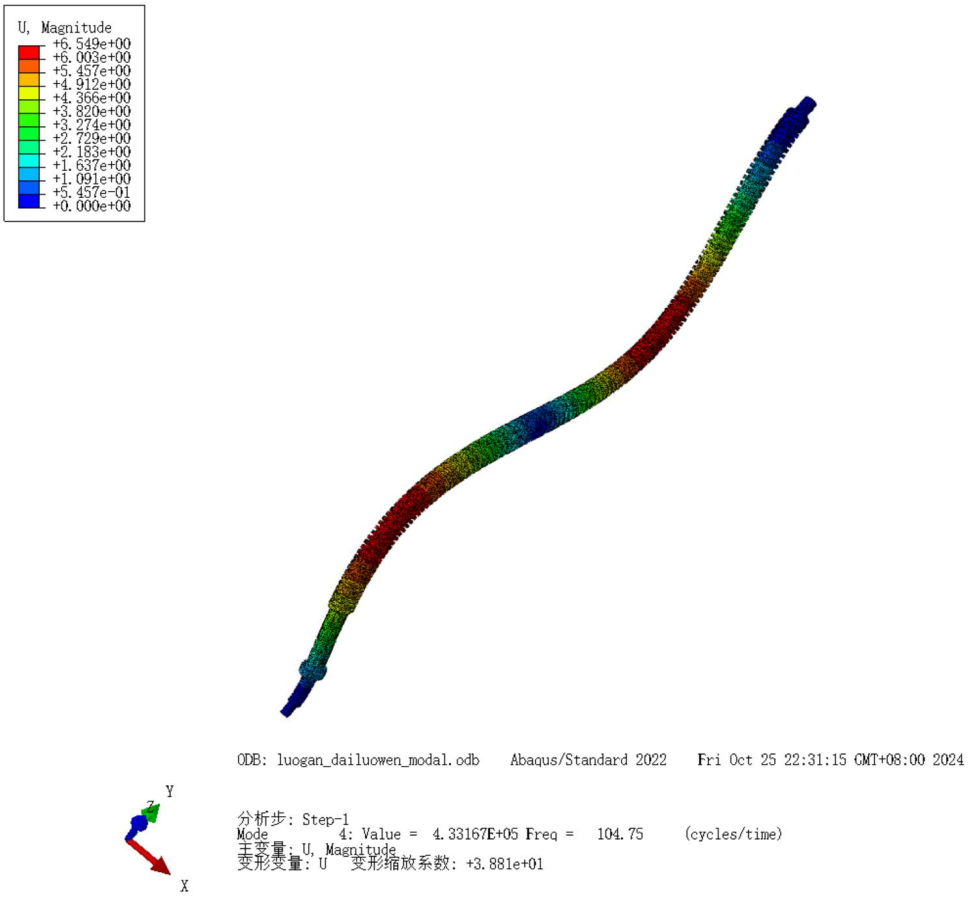

d: Fourth-order natural frequency of the screw

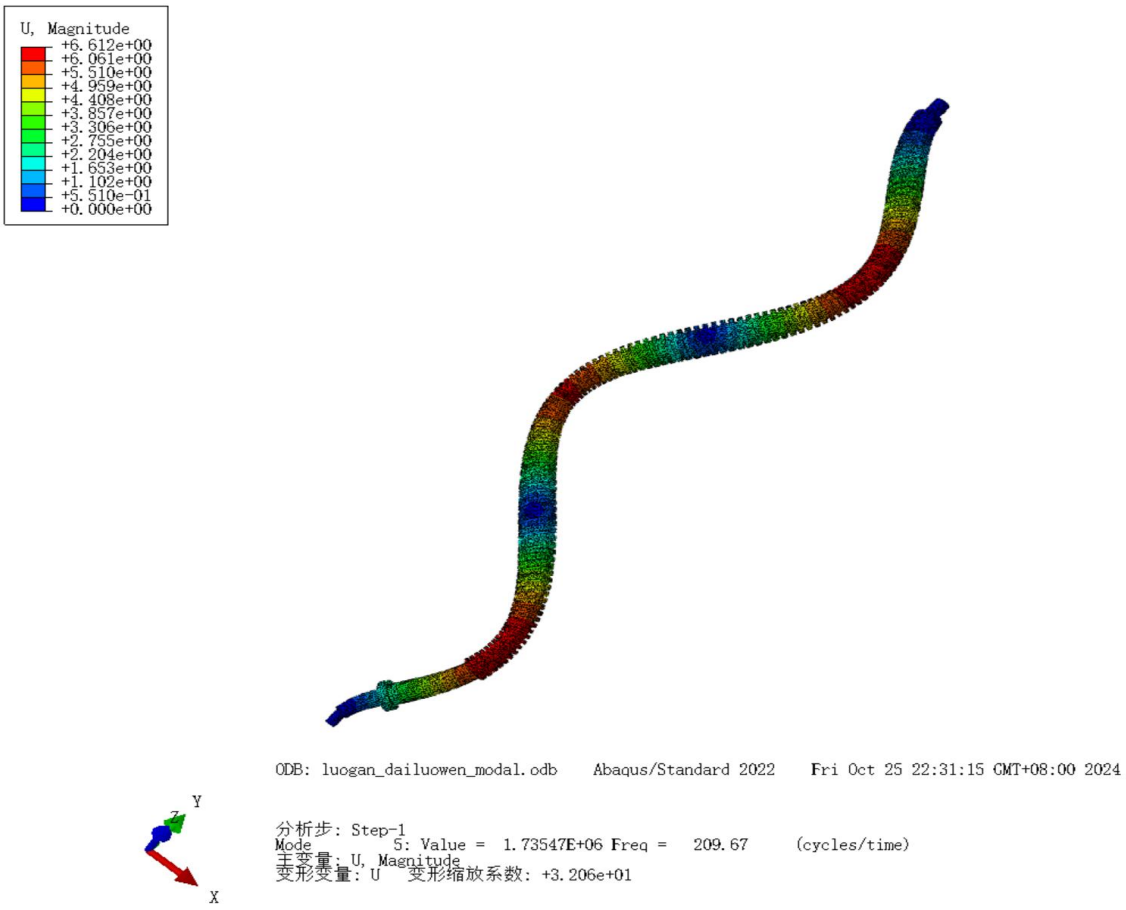

e: Fifth-order natural frequency of the screw

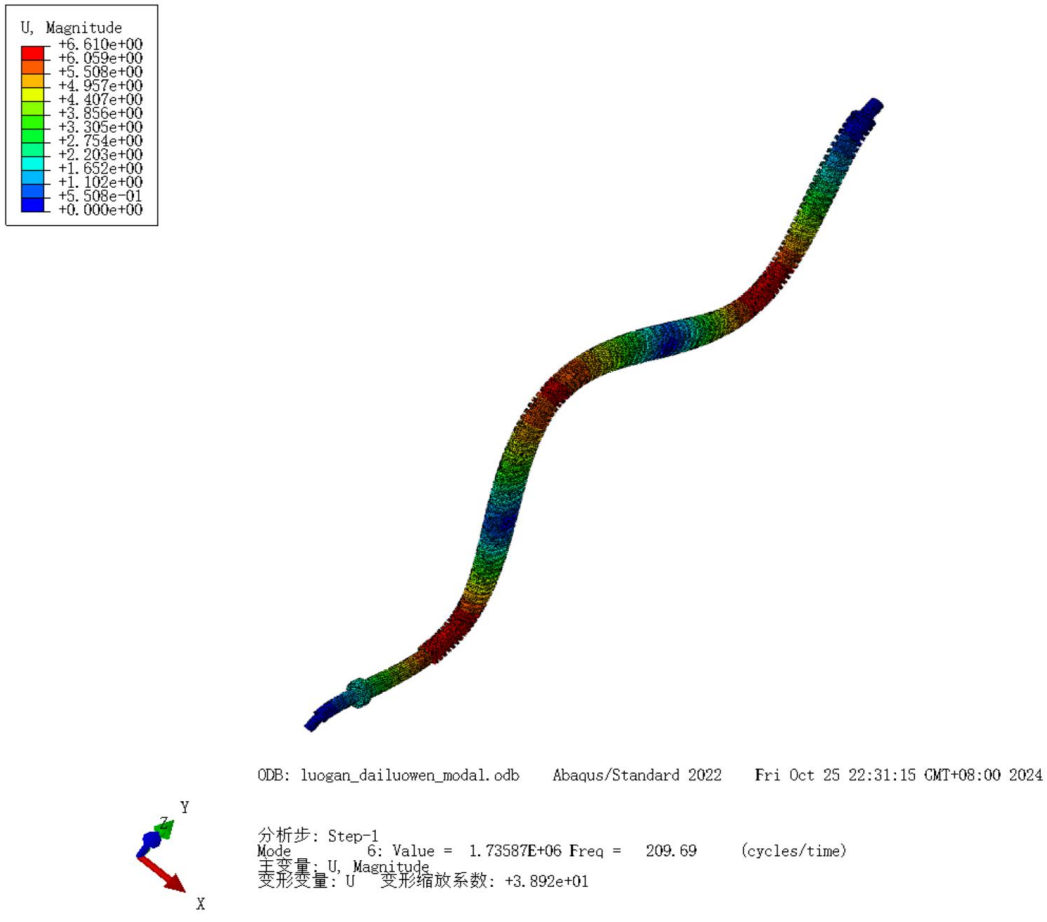

f: Sixth-order natural frequency of the screw

Figure 8: The first six modes of the screw

Due to the complete symmetry of the screw structure, the natural frequencies of rotation around the symmetrical plane and perpendicular to the symmetrical plane are equal, and the mode shapes are identical. According to the finite element analysis results, the first six natural frequencies of the screw are distributed in the range of 35 Hz to 210 Hz. The first and second natural frequencies are equal, with mode shapes corresponding to first-order bending deformations around the y-axis and x-axis. The third and fourth natural frequencies correspond to second-order bending deformations in both directions. The fifth and sixth natural frequencies correspond to third-order bending deformations in both directions.

4. Dynamic Harmonic Response Analysis of the Launch Device

4.1 Finite Element Modeling of the Entire Launch Device

The finite element model of the launch device consists of 875,989 nodes and 607,163 elements. In this study, the firing angle is set to 53°, with a direction angle of 0°. The overall model is shown in Figure 9.

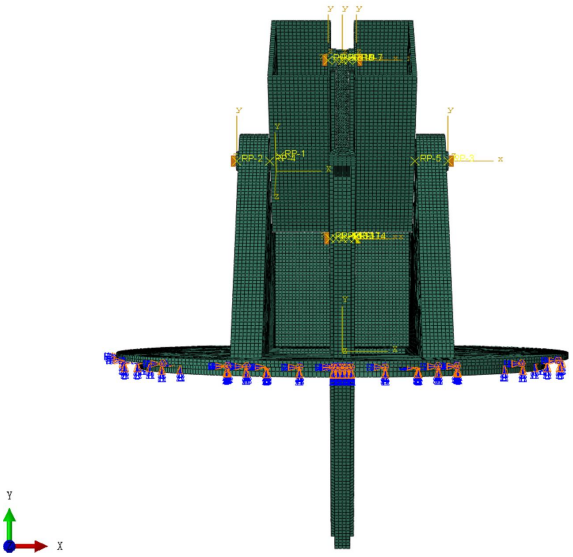

Figure 9: Finite Element Model of the Launching System as a Whole

By connecting the finite element models of the key components through contact surfaces [11], the contact and collision behavior of these components during the firing process can be effectively simulated. This is especially important for modeling the nonlinear contact phenomena of key components such as the launch box, bracket, and cradle. This approach helps to better simulate the dynamic response of the launch device under working conditions.

During the firing process of the launch device, the launch box experiences nonlinear impact forces, with the direction perpendicular to the bottom of the launch box. The pressure curve at the bottom of the chamber, denoted as *F*, can be obtained based on relevant parameters, as shown in Figure 10.

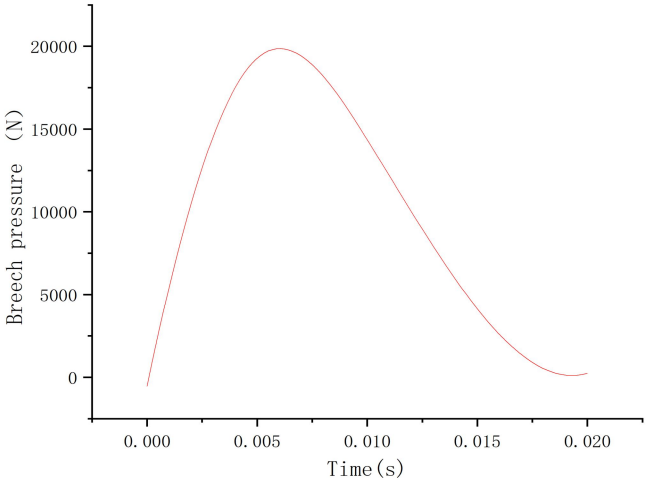

Figure 10: Breech pressure curve

It is assumed that the outer ring of the bracket remains fixed to the deck during the firing process, meaning that the displacement of the outer ring in all six degrees of freedom is constrained to zero. This approach effectively simplifies the complexity of load application in the finite element model. As shown in Figure 11, the red outer ring section represents the surface where fixed constraints are applied.

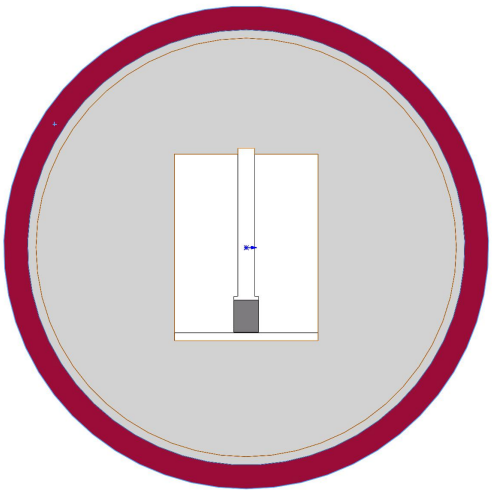

Figure 11: The part where the bracket is rigidly connected to the deck

4.2 Harmonic Response Analysis

The harmonic response analysis is performed on the entire launch device, which is connected by contact surfaces, with the boundary conditions and loads kept unchanged. Since the key components of the launch device have significant natural frequencies below 90 Hz, the frequency range selected for this study is 1-90 Hz, divided into 80 steps. Position constraints and excitations are applied. The harmonic response analysis is conducted using finite element analysis software, and the results are shown in Figure 12, Figure 13, and Figure 14.

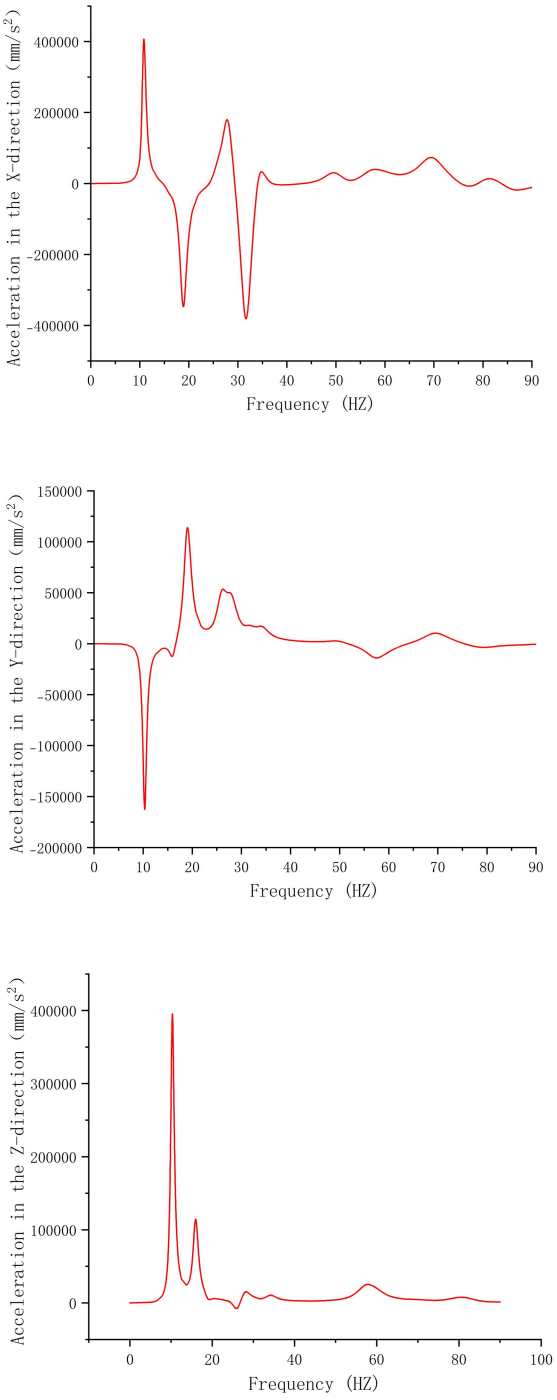

Figure 12: Harmonic response analysis of acceleration in the X, Y, and Z directions at the launch box opening

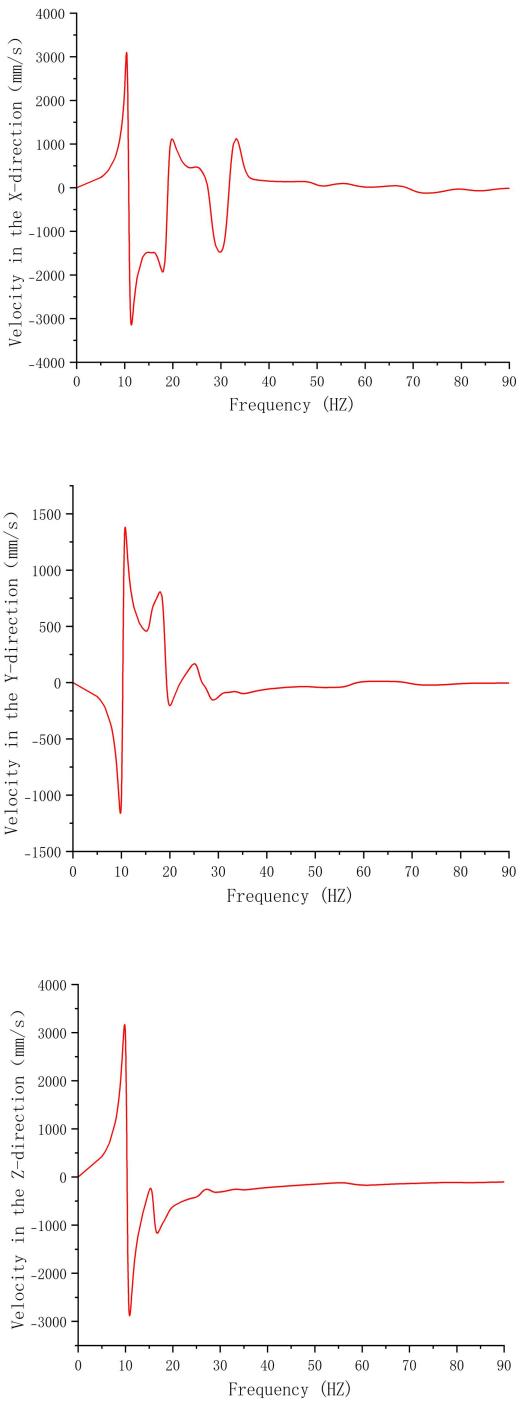

Figure 13: Harmonic response analysis of velocity in the X, Y, and Z directions at the launch box opening

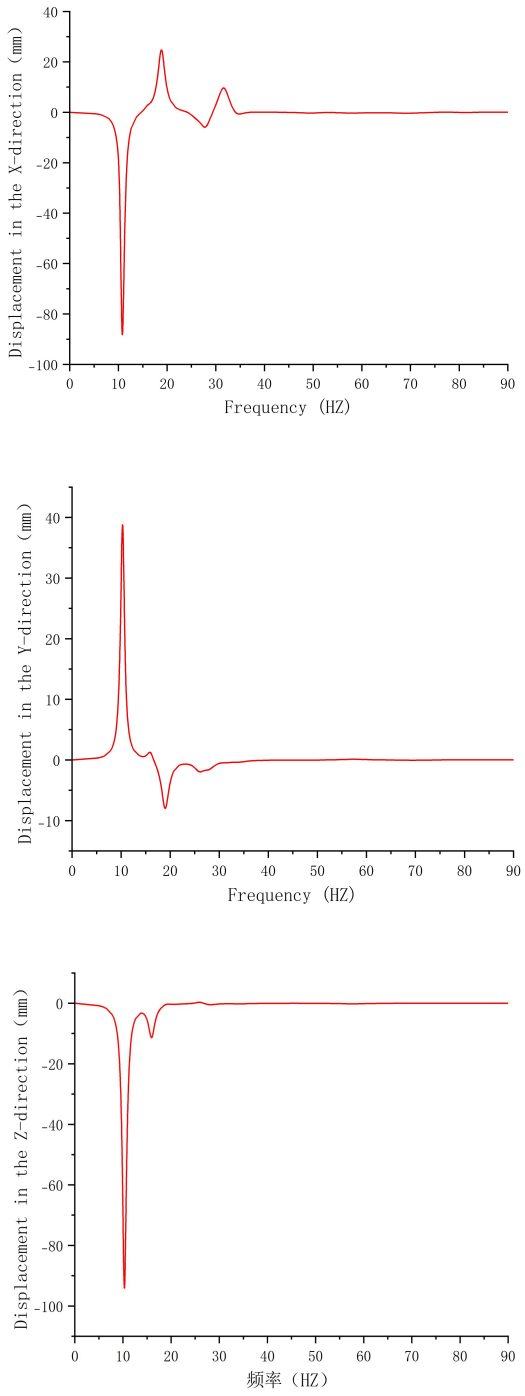

Figure 14: Harmonic response analysis of displacement in the X, Y, and Z directions at the launch box opening

From Figure 12, Figure 13, and Figure 14, it can be observed that the first, second, and fourth natural frequencies of the launch box, the second natural frequency of the bracket, and the first natural frequency of the screw are within the sensitive frequency range of the launch box mouth vibration. Therefore, reasonably matching the natural frequencies of the components of the launch device to avoid resonance is a crucial method for optimizing the design of the launch system and improving shooting accuracy.

5. Design Parameters and Response Calculation of the Response Surface

The natural frequency is closely related to the structural properties such as mass and stiffness, and is also influenced by the material properties. The material density can be adjusted to change the natural frequency of the structure.

Factor levels refer to the states of influencing factors, and selecting appropriate parameters is crucial to the optimization results. By analyzing the harmonic response results, the frequency range of the sensitive areas of the firing box mouth vibration in the firing system of the key components of the launch device is determined. Corresponding modal frequency factor level tables are designed, as shown in Table 5.

Table 5: Design parameter value level table

Level	Minimum Value	Middle Value	Maximum Value
Launch Box First Order Frequency	19.380	22.500	23.050
Bracket Second Order Frequency	21.440	22.950	24.140
Screw First Order Frequency	32.450	36.440	38.600

Through the Response Surface module in Design-Expert software, an orthogonal experimental design was conducted using the Box-Behnken method. After inputting the parameters from the level table of the simulation test parameters, a total of 17 orthogonal experimental schemes were obtained. Based on the orthogonal experimental design provided in the table, dynamic simulations were performed for each set of data to obtain the displacement response values in the x-direction and y-direction of the firing box mouth under different experimental schemes, as shown in Table 6.

Table 6: Dynamic simulation responses of each experimental scheme

	Factor 1	Factor 2	Factor 3	Response 1	Response 2
Run	A: Launch Box First Order Frequency	B: Bracket Second Order Frequency	C: Screw First Order Frequency	Launch Box Mouth X-Direction Displacement Response	Launch Box Mouth Y-Direction Displacement Response
	HZ	HZ	HZ	mm	mm
1	19.380	22.950	38.600	4.03052	1.72097
2	23.050	22.950	32.450	4.76888	1.96932
3	22.500	24.140	32.450	5.01352	1.92186
4	23.050	22.950	38.600	4.76597	1.96768
5	22.500	21.440	32.450	5.10655	1.89301
6	19.380	21.440	36.440	4.06268	1.70343
7	22.500	22.950	36.440	5.01907	1.91734
8	23.050	24.140	36.440	4.74497	1.9796
9	22.500	22.950	36.440	5.04117	1.92134
10	22.500	22.950	36.440	5.03089	1.91784
11	22.500	22.950	36.440	5.03987	1.91854
12	22.500	21.440	38.600	5.09503	1.89637
13	19.380	22.950	32.450	4.03622	1.71057
14	22.500	22.950	36.440	5.03047	1.91634
15	22.500	24.140	38.600	4.99775	1.92729
16	19.380	24.140	36.440	4.02991	1.7248
17	23.050	21.440	36.440	4.79831	1.94441

Table 6 lists a total of 17 experimental data sets, each corresponding to specific displacement response values in the x-direction and y-direction of the firing box mouth. The analysis results show that when the first-order natural frequency of the firing box is 22.5 Hz, the second-order natural frequency of the bracket is 21.440 Hz, and the first-order natural frequency of the screw is 32.45 Hz, the displacement response in the x-direction of the firing box mouth is maximized, with a value of 5.10655 mm. Conversely, when the first-order natural frequency of the firing box is 19.38 Hz, the second-order natural frequency of the bracket is 24.14 Hz, and the first-order natural frequency of the screw is 36.44 Hz, the displacement response in the x-direction of the

firing box mouth is minimized, with a value of 4.02991 mm. When the first-order natural frequency of the firing box is 23.05 Hz, the second-order natural frequency of the bracket is 24.140 Hz, and the first-order natural frequency of the screw is 36.44 Hz, the displacement response in the y-direction of the firing box mouth is maximized, with a value of 1.9796 mm. Conversely, when the first-order natural frequency of the firing box is 19.38 Hz, the second-order natural frequency of the bracket is 21.44 Hz, and the first-order natural frequency of the screw is 36.44 Hz, the displacement response in the y-direction of the firing box mouth is minimized, with a value of 1.70343 mm. This result highlights the importance of natural frequency matching, which has significant implications for the design optimization of the firing system.

5.1 Response Surface Results Analysis

In this chapter, using the Box-Behnken design method in Design-expert software, a response surface model was constructed between the modal frequencies of key components of the firing system and the firing box mouth response. The 17 sets of simulation data from Table 6 were input into the optimization analysis software, resulting in a second-order polynomial expression for the displacement responses in both directions of the firing box mouth, along with their variance analysis. In this context, A, B, and C represent the first-order frequency of the firing box, the second-order frequency of the cradle, and the first-order frequency of the screw, respectively.

$$\begin{aligned} x=&5.15+0.3657*A-0.0309*B-0.0041*C \\ &-0.0111*AB-0.0013*AC+0.0018*BC \\ &-0.7506*A^2+0.0107*B^2+0.0048*C^2 \end{aligned} \quad (1)$$

$$\begin{aligned} y=&1.82+0.1254*A+0.0134*B+0.0031*C \\ &+0.0031*AB-0.0026*AC+0.0006*BC \\ &+0.0271*A^2-0.0050*B^2-0.0017*C^2 \end{aligned} \quad (2)$$

Table 7: Variance analysis of the displacement in the X direction at the launch box opening

Source	Sum of Squares	df	Mean Square	F-value	p-value
Model	2.79	9	0.3105	1785.13	< 0.0001
A - Launch Box First Order Frequency	1.03	1	1.03	5911.63	< 0.0001
B - Bracket Second Order Frequency	0.0061	1	0.0061	35.05	0.0006
C - Screw First Order Frequency	0.0001	1	0.0001	0.6540	0.4453
AB	0.0006	1	0.0006	3.49	0.1040
AC	9.016E-06	1	9.016E-06	0.0518	0.8264
BC	0.0000	1	0.0000	0.0768	0.7896
A²	0.4896	1	0.4896	2815.10	< 0.0001
B²	0.0005	1	0.0005	2.63	0.1488
C²	0.0001	1	0.0001	0.4432	0.5269
Residual	0.0012	7	0.0002		
Lack of Fit	0.0009	3	0.0003	3.80	0.1150
Pure Error	0.0003	4	0.0001		
Cor Total	2.80	16			

Table 8: Variance analysis of the displacement in the Y direction at the launch box opening

Source	Sum of Squares	df	Mean Square	F-value	p-value
Model	0.1507	9	0.0167	4073.63	< 0.0001
A - Launch Box First Order Frequency	0.1208	1	0.1208	29384.28	< 0.0001
B - Bracket Second Order Frequency	0.0011	1	0.0011	276.56	< 0.0001
C - Screw First Order Frequency	0.0001	1	0.0001	15.11	0.0060
AB	0.0000	1	0.0000	11.69	0.0112
AC	0.0000	1	0.0000	8.15	0.0245
BC	1.430E-06	1	1.430E-06	0.3477	0.5739
A2	0.0006	1	0.0006	154.86	< 0.0001
B2	0.0001	1	0.0001	24.23	0.0017
C2	9.092E-06	1	9.092E-06	2.21	0.1806
Residual	0.0000	7	4.111E-06		
Lack of Fit	0.0000	3	4.836E-06	1.36	0.3759
Pure Error	0.0000	4	3.568E-06		
Cor Total	0.1508	16			

Equation (1) is the second-order polynomial fitting expression for the displacement response in the x-direction, and Equation (2) is the second-order polynomial fitting expression for the displacement response in the y-direction. Table 7 presents the variance analysis for the second-order polynomial fitting expression of the displacement response in the x-direction, and Table 8 presents the variance analysis for the second-order polynomial fitting expression of the displacement response in the y-direction.

Based on the variance analysis results for the displacement responses in both the x and y directions, the significance of the regression relationships between the natural frequencies of the firing box, cradle, and screw and the displacement response at the firing box mouth was determined using the P-value.
In the variance analysis for the x-direction displacement response at the firing box mouth:

The first-order frequency of the firing box has a highly significant effect on the x-direction displacement response ($P < 0.0001$).

The P-value for the second-order frequency of the cradle is < 0.001, indicating a highly significant effect on the x-direction displacement response.

The P-value for the first-order frequency of the screw is 0.4453, which is greater than 0.05, indicating that it does not significantly affect the x-direction displacement response.

The P-value for the squared term of the first-order frequency of the firing box is < 0.0001, showing a significant effect on

the x-direction displacement response.

The P-values for the interaction terms between the second-order frequency of the cradle and the first-order frequency of the screw, and other higher-order interaction terms, are greater than 0.05, indicating no significant effect on the x-direction displacement response.

The P-value for the lack of fit is greater than 0.05, indicating that the fitted x-direction displacement response aligns well with the actual x-direction displacement response, with minimal error.

In the variance analysis for the y-direction displacement response at the firing box mouth:

The P-values for the first-order frequency of the firing box and the second-order frequency of the cradle are both < 0.0001, showing that these two design factors have a highly significant effect on the y-direction displacement response.

The P-value for the first-order frequency of the screw is 0.006, greater than 0.005, indicating that this design factor does not significantly affect the y-direction displacement response.

The P-value for the squared term of the first-order frequency of the firing box is < 0.0001, showing a highly significant effect on the y-direction displacement response.

The P-value for the squared term of the second-order frequency of the cradle is 0.0017, indicating a significant effect on the y-direction displacement response.

The P-value for the squared term of the first-order frequency of the screw is 0.1806, greater than 0.05, showing no significant effect on the y-direction displacement response.

The P-values for the interaction terms between the first-order frequency of the firing box and the second-order frequency of the cradle, and between the first-order frequency of the firing box and the first-order frequency of the screw, are both < 0.05, indicating a significant effect on the y-direction displacement response.

The P-value for the interaction term between the second-order frequency of the cradle and the first-order frequency of the screw is greater than 0.05, indicating no significant effect on the y-direction displacement response.

The P-value for the lack of fit is 0.3759, which is much greater than 0.05, indicating that the fitted y-direction displacement response aligns well with the actual y-direction displacement response, with minimal error.

By comparing the fitted values with the dynamic simulation results, the fitted curves show a good fitting effect, with prediction points close to a straight line, as shown in Figure 15 and Figure 16.

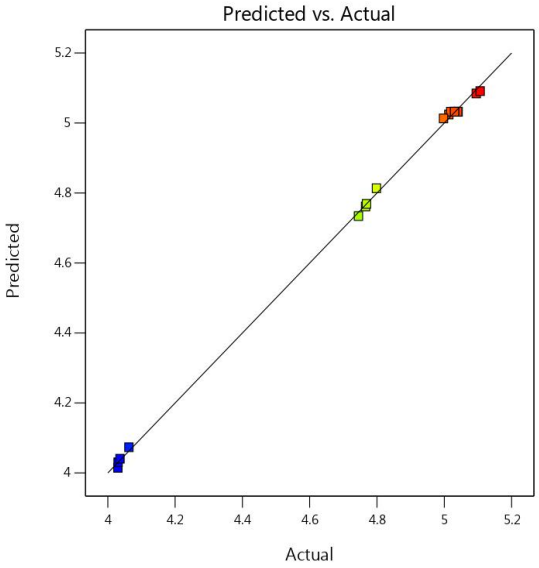

Figure 15: Comparison of predicted values and actual values in the X direction at the launch box opening

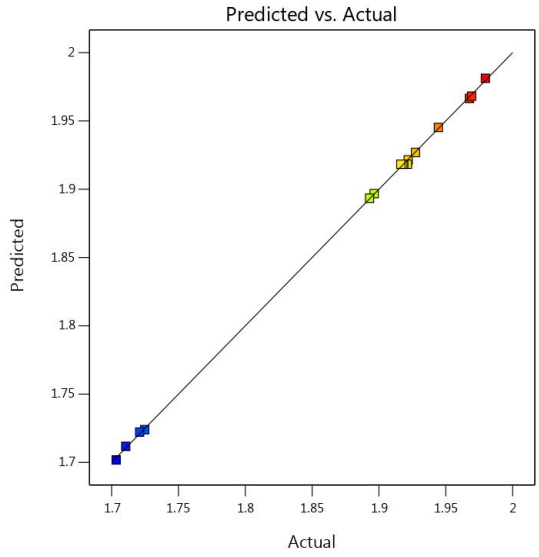

Figure 16: Comparison of predicted values and actual values in the Y direction at the launch box opening

5.2 Optimization Results Analysis

Through the use of the Optimization module in Design-expert software, the main objective of this study is to reduce the x-direction and y-direction displacement responses at the firing box mouth during the firing process. The specific optimization goal is to minimize the acceleration response at the firing box mouth (Minimize). The optimization analysis is performed based on the design optimization parameters and constraints listed in Table 9 to obtain the optimal design scheme.

After solving the optimization problem, 90 optimization results were obtained, with the optimal result shown in Table 10.

Table 9: The objective and constraint conditions of the optimization model

Name	Goal	Lower Limit	Upper Limit	Lower Weight	Upper Weight	Importance
A: Launch Box First Order Frequency	is in range	19.380	23.050	1	1	3
B: Bracket Second Order Frequency	is in range	21.440	24.140	1	1	3
C: Screw First Order Frequency	is in range	32.450	38.600	1	1	3
Launch Box x-direction Displacement Response	minimize	4.02991	5.10655	1	0.7	4
Launch Box y-direction Displacement Response	minimize	1.70343	1.9796	1	0.3	4

Table 10: Optimal Solutions for X and Y Direction Displacement Responses and Comprehensive Optimal Solution

First-order frequency of the launcher	Second-order frequency of the bracket	First-order frequency of the screw	X-direction displacement response at the launcher mouth	Y-direction displacement response at the launcher mouth	First-order frequency of the launcher
Optimal for x-direction displacement response	19.381	23.205	35.835	4.029	Optimal for x-direction displacement response
Optimal for y-direction displacement response	19.380	21.620	32.450	4.0678	Optimal for y-direction displacement response
Comprehensive optimal	19.380	24.139	32.450	4.0300	Comprehensive optimal

From the optimization results, the following conclusions can be drawn:

To minimize the x-direction displacement response at the firing box mouth, the first-order natural frequency of the firing box should approach the minimum value of the set frequency range, the second-order natural frequency of the bracket should approach the maximum value of the frequency range, and the first-order frequency of the screw should remain unchanged.

To minimize the y-direction displacement response at the firing box mouth, the first-order natural frequency of the firing box should approach the minimum value of the set frequency range, the second-order natural frequency of the bracket should approach the minimum value of the frequency range, and the first-order frequency of the screw should also approach the minimum value of the frequency range.

For the comprehensive optimization to achieve the best results, i.e., simultaneously reducing both the x-direction and y-direction displacement responses at the firing box mouth, the first-order natural frequency of the firing box should be reduced, the second-order natural frequency of the bracket should be increased, and the first-order natural frequency of the screw should be reduced. Given the limitations of the modal optimization for the firing box and screw, the second-order natural frequency of the bracket should be increased to optimize its vibration resistance, thereby reducing the displacement response at the firing box mouth during firing.

This frequency-based optimization matching approach enables the components of the firing system to work more collaboratively during firing, effectively reducing both lateral and longitudinal displacement responses and vibration during the firing process. These optimization results provide a theoretical basis for structural improvements to the firing system and contribute to enhancing the overall performance.

6. Conclusion

This paper introduces the basic principles of the Response Surface Method (RSM) and proposes the use of the Box-Behnken Design (BBD) to select sample points, thereby constructing design parameters, i.e., the approximate functional relationship between the natural frequencies of key components sensitive to the firing box mouth vibrations and the x-direction and y-direction displacement responses. The goal of the Response Surface Method is to model experimental data and find the relationship between input variables and output responses, enabling an effective evaluation of the impact of design parameters on system performance with fewer experiments. Through this method, the vibration characteristics of the firing box mouth can be systematically optimized, improving its shooting accuracy and stability.

Using the established response surface approximation model, the x-direction and y-direction displacement responses at the firing box mouth were optimized to achieve comprehensive optimal performance. This process determined the best frequency matching scheme, aiming to effectively reduce the x-direction and y-direction displacement responses at the firing box mouth through frequency matching. Furthermore, the optimization results provide an important reference for subsequent structural design and improvements, further advancing the performance enhancement of the firing system.

References

[1] Zeng Shengyu. Optimization Design Technology for Anti-Ship Missiles Based on Response Surface Approximation in Parallel Subspace [D]. Northwestern Polytechnical University, 2004.R. Caves, Multinational Enterprise and Economic Analysis, Cambridge University Press, Cambridge, 1982. (book style)

[2] Che Wenkan, Li Lixin, Wang Feng. Experimental Study on the Optimization of the Inner Ring Structure of Riveted Hub Bearing Units Based on Response Surface Method [J/OL]. Electromechanical Engineering, 1-10 [2024-11-14].

[3] Wang Yugang, Xiu Shichao. Multi-Objective Optimization Design of Motor Brackets Using Response Surface Method [J]. Mechanical Design and Manufacture, 2021(10): 42-44. K. Deb, S. Agrawal, A. Pratab, T. Meyarivan, "A Fast Elitist Non-dominated Sorting Genetic Algorithms for Multiobjective Optimization: NSGA II," KanGAL report 200001, Indian Institute of Technology, Kanpur, India, 2000. (technical report style)

[4] He H, Zhou J, Xu L, et al. Optimization of a novel lateral energy dissipation system for cable-stayed bridge with

short piers based on seismic vulnerability analysis [J]. Structures, 2024,70107700-107700.

[5] Yue, J. (2016). Modal Matching Analysis and Optimization of a Certain Naval Gun (Master's thesis). Nanjing University of Science and Technology.

[6] Cai, J., Liu, Z., Wang, G., et al. (2024). Optimization Design of the Auxiliary Tail Rope Device for the Winch Based on Response Surface Method. Journal of Engineering Design, 31(02),

[7] Song, Z. (2022). Research on Robust Design of Turbomachinery Engine Dynamics Based on Higher-Order Response Surface Method [Master's Thesis]. Nanjing University of Aeronautics and Astronautics.DOI:10.27239/d.cnki.gnhhu.2022.000210.

[8] Zuo, Y. (2022). Vibration Characteristics Analysis and Modal Matching Study of Key Components of Large-Caliber Naval Guns [Master's Thesis]. Harbin Engineering University. DOI: 10.27060/ d.cnki.ghbcu.2022.001811.

[9] Li, X., Wang, S., & Zhao, S. (2019). Study on the Influence of Solid Element Types on Simulation Results. Journal of Dalian Jiaotong University, 40(02), 76-79. DOI: 10.13291/j.cnki.djdxac.2019.02.017.

[10] Yang, J. (2020). Principles for Selecting Finite Element Mesh Elements. Henan Science and Technology, (17), 35-37.

[11] Fu, W., Lou, L., Gao, Z., et al. (2017). Theoretical Model of Normal Contact Stiffness and Damping for Mechanical Joints. Journal of Mechanical Engineering, 53(09), 73-82.